25. Oser, B. L., *Hawks Physiological Chemistry*, Mc Graw Hill, New York, 1979.
26. Griffith, O. W., Determination of glutathione and glutathione disulphide using glutathione reductase and 2-vinyl pyridine. *Anal. Biochem.*, 1980, **106**, 207–211.
27. Makela, P., Karkkainen, J. and Somersalo, S., Effect of glycine-betain on chloroplast ultrastructure, chlorophyll and protein content, and RuBPCO activities in tomato grown under drought or salinity. *Biol. Plant.*, 2000, **43**, 471–475.
28. Luna, C. M., Gonzalez, C. A. and Trippio, V. S., Oxidative stress caused by excess copper in oat leaves. *Plant Cell Physiol.*, 1994, **35**, 11–15.
29. Gallego, S. M., Benavioes, M. P. and Tomaro, M. L., Effect of heavy metal ions on sunflower leaves – Evidence for involvement of oxidative stress. *Plant Sci.*, 1996, **121**, 151–159.
30. Panda, S. K. and Patra, H. K., Does chromium(III) produce oxidative stress in excised wheat leaves? *J. Plant Biol.*, 2000, **11**, 105–110.
31. Salt, D. E., Blaylock, M., Kumar, P. B. A. N., Dushenkov, E., Ensley, B. B., Chet, I. and Raskin, I., Phytoremedation: A novel strategy for removal of toxic metals from environment using plants. *Biotechnology*, 1995, **13**, 468–474.
32. Jiang, W., Lin, D. and Hon, W., Hyperaccumulation of lead by roots, hypocotyls and shoots of *Brassica juncea*. *Biol. Plant.*, 2000, **43**, 603–606.
33. Dietz, K. J., Baier, M. and Kramer, U., Free radicals and reactive oxygen species as mediator of heavy metal toxicity in plants. *Heavy Metal Stress in Plants. From Molecules to Ecosystem* (eds Prasad, M. N. V. and Hagemeyer, J.), Springer-Verlag, Berlin, 1999, pp. 73–79.
34. Levine, A., Tenhaken, R., Dixon, R. and Lamb, C., H_2O_2 from the oxidative brust orchestrates the plant hypersensitive disease resistance receptors. *Cell*, 1994, **79**, 583–593.
35. Halliwell, B. and Gutteridge, J. M. C., *Free Radical in Biology and Medicine*, Clarendon Press, Oxford, 1988, pp. 1–51.
36. Vranova, E., Inze, D. and Van Breusegem, F., Signal transduction during oxidative stress. *J. Exp. Bot.*, 2002, **53**, 1227–1236.
37. Sandalio, L. M., Dalurzo, H. C., Gomez, M., Romero-Puertas, M. C. and del Rio, L. A., Cadmium-induced changes in growth and oxidative metabolism of pea plants. *J. Exp. Bot.*, 2001, **52**, 2115–2126.
38. Fryer, M. J., The antioxidant effect on thylakoid vitamin E (*a*-tocopherol). *Plant Cell Environ.*, 1992, **15**, 381–392.
39. Foyer, C. H., Ascorbic acid. *Antioxidants in Higher Plants* (eds Alscher, R. G. and Hess, J. L.), CRC Press, Boca Raton, 1993, pp. 31–58.
40. Alscher, R. G., Donahue, J. L. and Cramer, C. L., Reactive oxygen species and antioxidants. Relationship in green cells. *Plant Physiol.*, 1997, **100**, 224–233.
41. Noctor, G. and Foyer, C. H., Ascorbate and glutathione: Keeping active oxygen under control. *Annu. Rev. Plant Physiol. Plant Mol. Biol.*, 1998, **49**, 250–279.
42. Baryla, A., Laborde, C., Montillet, J. E., Triantaphylides, C. and Changvardiefe, P., Evaluation of lipid peroxidation as a toxicity bioassay for plants exposed to copper. *Environ. Pollut.*, 2000, **109**, 131–136.

ACKNOWLEDGEMENTS. We thank Dr Sudip Dey, Sophisticated Analytical Instrument Facilities, North Eastern Hill University, Shillong for Transmission Electron Microscopy facility.

Received 6 December 2003; revised accepted 24 March 2004

Trichromatic sorting of *in vitro* regenerated plants of gladiolus using adaptive resonance theory

Mahendra, V. S. S. Prasad and S. Dutta Gupta*

Department of Agricultural and Food Engineering, Indian Institute of Technology, Kharagpur 721 302, India

A machine vision system is described to sort the regenerated plants of gladiolus into groups using trichromatic features of leaves. The machine vision system consisted of a scanner, image analysis software and an adaptive resonance theory neural network. Leaf attributes extracted from the image histograms and used for network classification are the mean brightness, grey-scale level and the maximum pixel count. The system was able to sort the regenerated plants into two distinct groups based on the photometric behaviour. Vigilance parameter had a significant effect on grouping. The approach may provide a means of selecting plants suitable for *ex vitro* transfer and also helps in quality control of commercial micropropagation.

THE primary goal of commercial micropropagation is to achieve a large number of genetically identical, physiologically uniform and developmentally normal plants with the ability to survive upon transfer to *ex vitro* conditions in a relatively short period of time. However, one of the major problems in commercialization of the micropropagation technique is the poor survival of regenerated plants upon *ex vitro* transfer. The intrinsic quality of the regenerated plants is largely responsible for its survival during the period of acclimatization. Various approaches such as photoautotrophic micropropagation[1], use of raft and immersion culture with or without growth retardants[2–4] and machine vision system have been adopted to reduce the costs and improve plant survival.

In plant tissue culture system, machine vision has found applications in growth determination of suspension cultures[5] and regenerated whole plants[6], somatic embryo sorting[7], automatic shoot separation[8] and selection of embryogenic cultures[9]. The purpose of this work is to test the hypothesis whether regenerated plants can be sorted out into groups based on their photometric behaviour using image analysis system coupled with neural network algorithm. It is well understood that the successful clustering of regenerated plants gives an opportunity to identify and select plants amenable for *ex vitro* survival.

In the present communication, we describe a method to project the trichromatic variations of regenerated plants and sort them out into groups using adaptive resonance theory (ART2). ART2 is a neural network algorithm deri-

*For correspondence. (e-mail: sdg@agfe.iitkgp.ernet.in)

ved from adaptive resonance theory[10]. It is a clustering algorithm which clusters a given set of input patterns into some groups in an unsupervised manner.

Sprouted shoots of *Gladiolus hybridus* Hort. cv. Wedding Bouquet were surface sterilized with 5% sodium hypochlorite with two to three drops of Tween-20 for 15 min and washed thoroughly with sterile distilled water. Innermost leaves were dissected out, cut into small pieces and cultured on Murashige and Skoog (MS) medium[11] containing 2 mg/l *a*-naphthaleneacetic acid (NAA), 3% sucrose and 0.8% agar for callus induction. Compact calluses thus obtained were transferred to MS medium supplemented with 0.2 mg/l NAA and 2.0 mg/l benzyladenine for differentiation of meristematic clusters as described previously[12]. For proliferation of shoots and complete plantlet development, meristematic clusters were placed on GA-9 vessel (Osmotek, Israel) with 50 ml of MS medium containing 0.5 mg/l NAA and incubated for three weeks. The pH of the medium was adjusted to 5.6 before autoclaving at 121°C for 15 min. All the cultures were kept at 16 h photoperiod (irradiance of 60 μmol m^{-2} s^{-1}), temperature of 25°C, and relative humidity of 50%. There were five replications each with five clusters per vessel.

The outermost expanded leaves of the regenerated plants were excised randomly from each cluster, washed and blotted dry. They were then scanned using Hewlett Packard flatbed scanner series 11.0 under constant luminosity to acquire the digitized images. The images were saved as Adobe Photoshop (*.psd) format with a desktop resolution of 16 bits per pixel having 256 grey-scale levels. The pixel properties of the images were evaluated using Adobe Photoshop 7.0 software. A fixed number of pixels (4 × 4) were selected from the median portion of leaves to obtain histograms. From the luminosity and trichromatic components of the pixels, the mean brightness, grey-scale level for the maximum pixel count and maximum pixel count were recorded.

The training set comprised 25 leaf images each having its origin from a regenerated plant per cluster. Leaves collected from five clusters in a vessel were numbered 1 to 5. Attributes of leaf image 1 of each vessel were fed serially to the algorithm. Twelve attributes for each leaf input pattern were subjected to ART2-based classification using vigilance parameter value of 0.59 to 0.99. A program based on 'C' language has been developed using ART2 algorithm to categorize the leaf images, the outcome of which is presented in the form of groups.

The component steps of the machine vision system along with the structural architecture of ART2 algorithm are presented in Figure 1. The description that follows is intended to summarize and provide the readers with a generalized outline of the ART2 network principles. *F1* layer has been divided into six sub-layers; *w*, *x*, *u*, *v*, *p* and *q* containing both feed-forward and feed-back connections to deal successfully with the analogue patterns in ART2. *G* is a gain control unit that sends nonspecific inhibitory signals to each unit on the layer it feeds. All sub-layers on *F1*, as well as the *r* layer of the orienting subsystem, have the same number of units. Individual sub-layers on *F1* are not fully interconnected, with the exception of the bottom-up connections to *F2* and the top-down connections from *F2*.

Summary of the algorithm for ART2 along with its exemplified numerical interpretation and constraints is as follows:

$a, b > 0$

$0 \le d \le 1$

$c * d/(1 - d) \le 1$

$0 \le q \le 1$

$0 \le r \le 1$

$e < < 1$.

Firstly, top-down weights are all initialized to zero

$$z_{ij}(0) = 0.$$

Bottom-up weights are initialized according to

$$z_{ji}(0) \le 1/\{(1 - d) * \sqrt{M}\}.$$

Individual quantity values vary according to the sub-layer being considered.

For example, in case of cluster classification an input vector $\boldsymbol{I}$ is defined as

$$\boldsymbol{I} = \{231.88, 235.0, 5.0, 230.88, 235.0, 3.0, 234.19, 237.0, 4.0, 222.25, 222.0, 3.0\}.$$

The following equations summarize the activities of the six sub-layers on *F1*

$$w_i = I_i + a * u_i,$$
$$x_i = w_i/(e + \|\boldsymbol{w}\|),$$
$$v_i = f(x_i) + b * f(q_i).$$

The contrast enhancement that takes place on *F1* is determined by $f(x)$:

$$f(x) = \begin{cases} 0 & 0 \le x \le q \\ x & x > q \end{cases},$$

where q is a positive constant less than one.

$$u_i = v_i/(e + \|\boldsymbol{v}\|),$$
$$p_i = u_i + \Sigma\, q(y_j) * \boldsymbol{z_{ij}},$$
$$q_i = p_i/(e + \|\boldsymbol{p}\|).$$

Various constant values are chosen as $a = 10$; $b = 10$; $c = 0.1$; $d = 0.8$; $q = 0.0001$.

The parameter e is then typically set to a positive number considerably less than 1,

$$e = 0.000001.$$

The degree to which the system discriminates between different classes of input patterns and the granularity with which input patterns are classified by the network rely on the value of the vigilance parameter chosen. Here, for example, the value of vigilance parameter is set to r =

0.999. Applying input pattern $\boldsymbol{I}$ to w layer of $F1$, the output of this layer is

$$||\boldsymbol{w}|| = 653.663466.$$

This is further propagated to the $\boldsymbol{v}$ sub-layer, $\boldsymbol{u}$ sub-layer and $\boldsymbol{p}$ sub-layer and the output is as follows:

$$||\boldsymbol{v}|| = 1,\ ||\boldsymbol{u}|| = 0.999999,\ ||\boldsymbol{p}|| = 0.999999.$$

The activities of the nodes on the r layer of the orienting subsystem is given by the following equation,

$$r_i = u_i + c * p_i/(e + ||\boldsymbol{u}|| + ||\boldsymbol{p}||).$$

The value of the above expression is $||\boldsymbol{r}|| = 0.999999$.

In the matching process the two sub-layers which take part are $\boldsymbol{p}$ and $\boldsymbol{u}$. During learning, the activity of the units on the $\boldsymbol{p}$ layer simultaneously changes as top-down weights change on the $\boldsymbol{p}$ layer. The $\boldsymbol{u}$ layer remains stable during this process; therefore including it in the matching process prevents the occurrence of a reset while learning of a new pattern that is underway. The condition for reset is

$$r/(e + ||\boldsymbol{r}||) > 1,$$

and the value of the expression for the given input pattern is

$$r/(e + ||\boldsymbol{r}||) = 0.999/(0.000001 + 0.999999) = 0.9990.$$

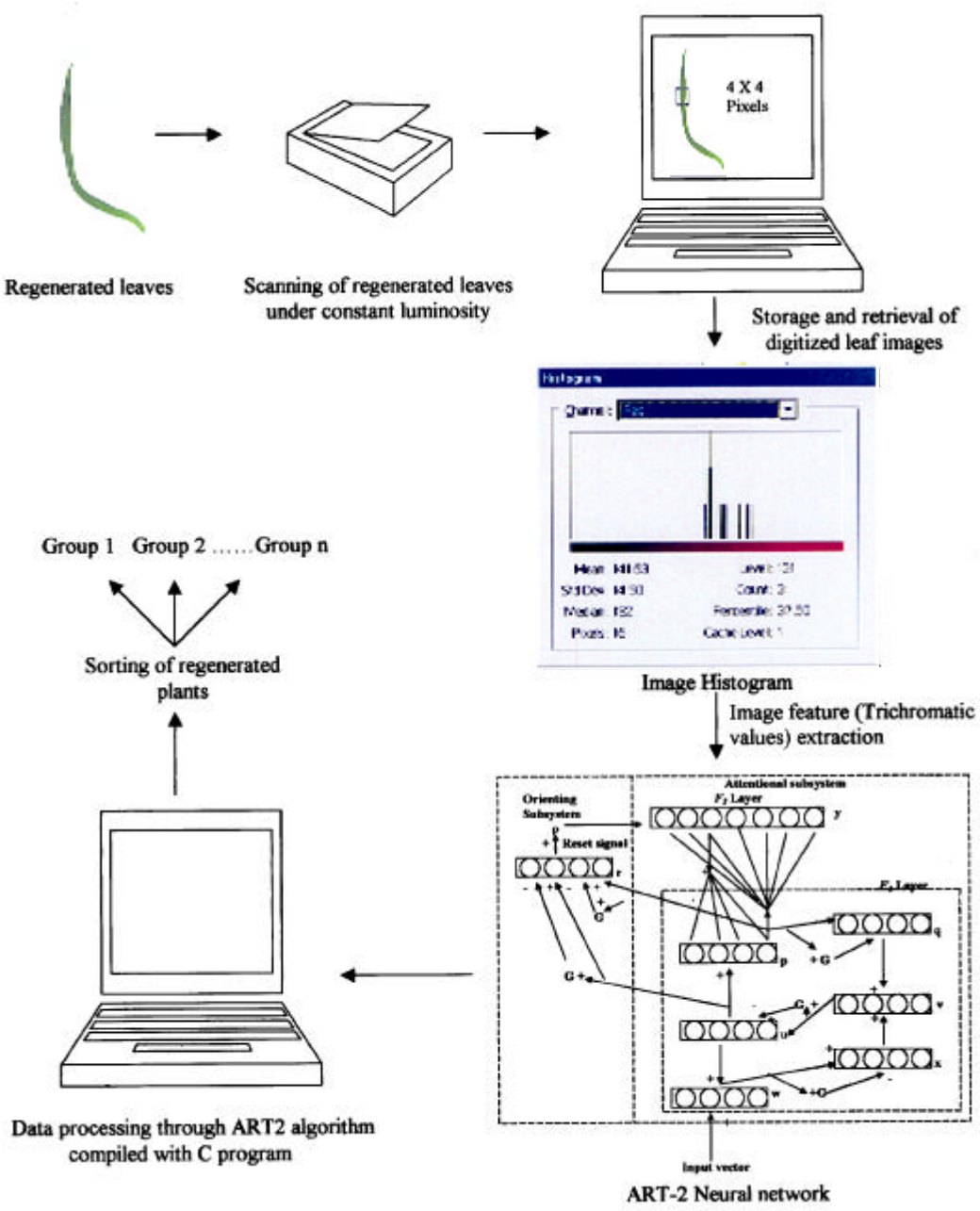

Figure 1. Component steps of machine vision analysis for sorting of *in vitro* regenerated plants into groups.

Where there is no reset, the weights have been modified as and when resonance has been established. Output of the *p* sub layer is then propagated to the *F2* layer. The net inputs to *F2* were calculated as

$$T_j = \sum_{i=1}^{M} (p_i * z_{ji}),$$

where *M* is the number of units in each *F1* sub-layer. The bottom-up weights and top-down weights were finally modified on the winning *F2* node.

Luminosity and trichromatic features at RGB regions of 25 digitized leaf images used for training the network are presented in Table 1. Input patterns of 13 leaf images used as test set are given in Table 2. Initially, input patterns of the training set were subjected to ART2 algorithm-based classification. The ART2 model was developed

Table 1. Luminosity and trichromatic features of training set extracted from digitized leaf images

						Trichromatic features								
			Luminosity			Red			Green			Blue		
Culture vessel no.	Leaf no.	Input pattern no.	Mean brightness	Grey level	Pixel count	Mean brightness	Grey level	Pixel count	Mean brightness	Grey level	Pixel count	Mean brightness	Grey level	Pixel count
1	1	1	231.88	235.0	5.0	230.88	235.0	3.0	234.19	237.0	4.0	222.25	222.0	3.0
	2	6	220.94	222.0	3.0	220.88	219.0	4.0	223.75	219.0	3.0	207.00	208.0	3.0
	3	11	210.63	223.0	2.0	216.81	214.0	3.0	213.06	218.0	2.0	181.06	173.0	2.0
	4	16	224.75	224.0	4.0	223.19	225.0	3.0	228.94	228.0	5.0	206.88	211.0	2.0
	5	21	223.44	224.0	5.0	221.38	222.0	3.0	227.81	227.0	5.0	204.19	202.0	4.0
2	1	2	185.25	196.0	2.0	190.44	192.0	3.0	215.63	224.0	2.0	8.69	0.0	7.0
	2	7	196.75	193.0	2.0	199.94	204.0	2.0	220.00	221.0	2.0	62.00	0.0	2.0
	3	12	180.31	187.0	2.0	184.40	195.0	2.0	196.81	193.0	3.0	80.44	0.0	2.0
	4	17	193.25	207.0	2.0	195.56	212.0	2.0	222.56	233.0	2.0	29.81	0.0	8.0
	5	22	170.94	173.0	3.0	173.63	181.0	2.0	201.38	203.0	3.0	0.38	0.0	14.0
3	1	3	199.38	195.0	2.0	205.38	220.0	2.0	215.33	214.0	2.0	98.88	157.0	2.0
	2	8	177.69	173.0	2.0	180.00	190.0	2.0	199.19	188.0	3.0	55.69	59.0	2.0
	3	13	171.50	224.0	2.0	174.38	137.0	2.0	193.13	208.0	2.0	48.75	0.0	9.0
	4	18	181.19	173.0	2.0	182.19	194.0	2.0	210.50	196.0	3.0	20.94	0.0	12.0
	5	23	171.88	168.0	2.0	176.25	174.0	2.0	200.63	197.0	2.0	5.88	0.0	11.0
4	1	4	185.38	175.0	2.0	187.44	192.0	2.0	192.81	186.0	2.0	139.19	149.0	2.0
	2	9	192.31	193.0	4.0	190.94	198.0	2.0	210.25	211.0	3.0	99.56	122.0	1.0
	3	14	181.06	177.0	3.0	189.94	202.0	3.0	204.63	189.0	2.0	30.56	0.0	9.0
	4	19	239.31	249.0	3.0	242.38	255.0	4.0	246.88	255.0	5.0	190.50	199.0	3.0
	5	24	187.38	165.0	2.0	204.50	215.0	2.0	195.31	188.0	2.0	97.00	86.0	2.0
5	1	5	210.63	219.0	2.0	212.06	216.0	3.0	212.38	220.0	2.0	198.38	207.0	2.0
	2	10	232.88	239.0	2.0	234.06	242.0	2.0	237.75	245.0	2.0	202.31	209.0	2.0
	3	15	215.25	213.0	4.0	218.25	217.0	4.0	222.56	220.0	3.0	168.19	174.0	3.0
	4	20	230.88	234.0	2.0	234.00	226.0	4.0	234.13	237.0	3.0	204.63	207.0	3.0
	5	25	214.19	222.0	2.0	215.00	209.0	3.0	219.75	227.0	2.0	182.56	182.0	2.0

Table 2. Leaf image parameter of test set

					Trichromatic features								
		Luminosity			Red			Green			Blue		
Leaf no.	Input pattern no.	Mean brightness	Grey level	Pixel count	Mean brightness	Grey level	Pixel count	Mean brightness	Grey level	Pixel count	Mean brightness	Grey level	Pixel count
1	26	94.25	94.0	3	60.94	63.0	2	128.75	132.0	3	0.00	0.0	0
2	27	165.94	152.0	2	156.13	178.0	2	181.19	166.0	2	111.56	110.0	8
3	28	189.69	183.4	2	176.19	171.0	2	210.44	112.0	2	115.00	115.6	2
4	29	174.94	178.5	3	159.56	161.0	4	201.63	203.0	3	72.31	59.0	2
5	30	197.56	187.0	3	189.00	180.0	3	231.56	226.5	2	38.94	72.5	1
6	31	180.38	177.0	10	165.75	153.0	12	204.00	200.0	16	95.63	102.0	14
7	32	126.00	133.0	5	119.25	123.0	3	146.69	152.0	2	51.44	60.0	3
8	33	146.31	158.0	3	138.38	137.3	2	160.00	171.0	3	98.69	111.0	4
9	34	144.56	150.0	2	137.13	142.0	3	157.81	160.0	2	93.19	75.0	3
10	35	179.38	179.0	3	163.88	161.0	3	207.13	207.0	4	72.38	63.0	5
11	36	179.44	178.2	3	171.19	171.0	6	190.44	197.0	4	141.94	141.0	3
12	37	157.94	151.0	2	149.69	149.0	2	171.56	176.0	2	107.75	121.0	2
13	38	149.56	168.0	3	138.94	121.4	2	169.69	182.0	3	70.00	68.0	2

Table 3. Distribution and grouping of regenerated leaves of gladiolus by ART2 algorithm. Values represent leaf input pattern number

Training set (culture vessel no.)	Vigilance parameter			
	0.999		0.985	
	Group A	Group B	Group A	Group B
1	1, 6, 16, 21	11	1, 6, 11, 16, 21	–
2	7	2, 12, 17, 22	–	2, 7,12, 17, 22
3	13	3, 8, 18, 23	3	8, 13, 18, 23
4	4, 9, 19	14, 24	4, 9, 24	19, 14
5	5, 15, 20, 25	10	5, 10, 15, 20, 25	–
Test set	26, 27, 33, 36, 37	28, 29, 30, 31, 32, 34, 35, 38	NT*	NT*

* Not tested.

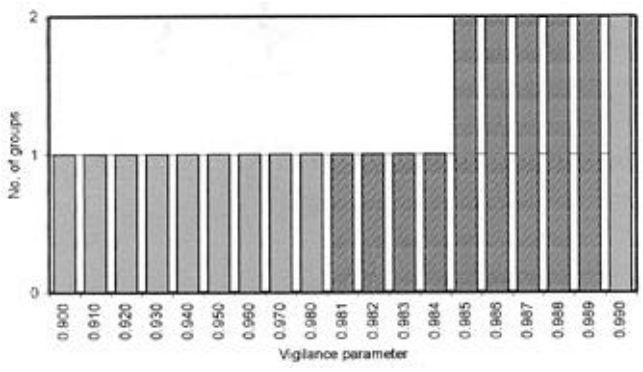

Figure 2. Effect of vigilance parameter on the number of groups generated by ART2.

for clustering analogue input patterns and was found to be most suitable in biological systems compared to other clustering methods such as hierarchical clustering, *K*-means algorithm and self-organizing maps[13]. The effect of vigilance parameter (VP) values was evaluated with increasing magnitude from 0.59 to 0.99. Figure 2 shows the number of groups generated under various VPs. The number of generated groups increased from 1 to 2 with the range over 0.985. This may be due to the 'mismatch reset' procedure of the algorithm facilitating the generation of new group. However, there was a difference in the grouping pattern with VP values of 0.985 and 0.99, though both the values resulted in two groups. With a VP of 0.985, the leaves of vessel numbers 1, 2 and 5 were categorized into a single group (either Group A for leaves of vessels 1 and 5 or group B for leaves of vessel 2) and the rest into two groups. VP of 0.99 classified the leaves of all vessels into two distinct groups, A and B, depicting efficient segregation of leaves based on image properties (Table 3).

To check the efficiency of the learning process, input patterns of the test set images were then classified with ART2 algorithm after training with a VP value of 0.99. All the 13 leaves were sorted into two groups, five in group A and the rest in group B (Table 3). The test leaf input pattern did not result in any variation in the grouping pattern. Similarity in grouping pattern between the training and test set data indicates the efficiency of network classification and its ability to recognize the invariant properties of domains. Furthermore, class separability is retained by the algorithm even with a 13-set data, indicating system validity with a small data set.

It appears that there exists variation among the regenerated plants at least in photometric behaviour. However, the variations reflected in altered colour spectrum of the leaves of regenerated plants may not parallel with 'somaclonal variation' described by Larkin and Scowcroft[14]. Leaves having maximum similarity in terms of inherent pixel properties fall in a particular group. Since the input patterns were obtained from the digitized images under constant luminosity and fixed number of pixels, the degree of error in classification is significantly minimized. Thus, on the basis of photometric features it is possible to group the regenerated plants. In plant tissue culture system, the use of trichromatic colours has only been restricted in the selection of sugarcane embryogenic callus[9]. The analysis was based on frequency distribution of brightness of the trichromatic colours, red, green and blue. This is a report on the application of adaptive resonance theory of artificial neural network (ANN) to successfully group the regenerated plants. Earlier, ANN has been used to monitor biomass evaluation in plant cell culture[15] and to estimate shoot length of regenerated rice[16].

In conclusion, the present work describes an approach to sort the regenerated plants of gladiolus into groups based on trichromatic features and analysis of data using adaptive resonance theory. Biological validation of grouping of regenerated plants, i.e. which group of plants is more suitable to *ex vitro* transfer remains to be investigated. However, the approach may provide a means of reliable and objective measurement for selecting plants amenable for *ex vitro* survival and quality control in commercial micropropagation.

1. Zobayed, S. M. A., Afreen, F., Kubota, C. and Kozai, T., Large-scale photoautotrophic micropropagation in a scaled-up vessel. In *Molecular Breeding of Woody Plants* (eds Morohoshi, N. and Komamine, A.), 2001, pp. 345–354.
2. Teng, W. L., Regeneration of *Anthurium* adventitious shoots using liquid or raft culture. *Plant Cell Tiss. Org. Cult*., 1997, **49**, 153–156.
3. Alvard, D., Cote, F. and Teisson, C., Comparison of methods of liquid medium culture for banana micropropagation. *Plant Cell Tiss. Org. Cult*., 1993, **32**, 55–60.
4. Ziv, M., Ronen, G. and Raviv, M., Proliferation of meristematic clusters in disposable presterilized plastic bioreactors for the large-scale micropropagation of plants. *In Vitro Cell. Dev. Biol. – Plant*, 1998, **34**, 152–158.
5. Ibaraki, Y. and Kenji, K., Application of image analysis to plant cell suspension cultures. *Comput. Electron. Agric.*, 2001, **30**, 193–203.
6. Smith, M. A. L., Spomer, L. A., Meyer, M. J. and McClelland, M. T., Non-invasive image analysis evaluation of growth during plant micropropagation. *Plant Cell Tiss. Org. Cult*., 1989, **19**, 91–102.
7. Ibaraki, Y., Image analysis for sorting somatic embryos. In *Somatic Embryogenesis in Woody Plants* (ed. Jain, S. M.), Kluwer, Netherlands, 1999, vol. 4, pp. 169–188.
8. Wang, Z., Heinemann, P. H., Walker, P. N. and Heuser, C., Automated micropropagated sugarcane shoot separation by machine vision. *Trans. ASAE*., 1999, **42**, 247–254.
9. Honda, H., Ito, T., Yamada, J., Hanai, T., Matsuoka, M. and Kobayashi, T., Selection of embryogenic sugarcane callus by image analysis. *J. Biosci. Bioeng*., 1999, **87**, 700–702.
10. Carpenter, G., A. and Grossberg, S., ART2: Stable self-organization of pattern recognition codes for analog input patterns. *Appl. Opt*., 1987, **26**, 4919–4930.
11. Murashige, T. and Skoog, F., A revised medium for rapid growth and bioassays with tobacco tissue cultures. *Physiol. Plant*., 1962, **15**, 473–497.
12. Dutta Gupta, S. and Datta, S., Antioxidant enzyme activities during *in vitro* morphogenesis of gladiolus and the effect of application of antioxidants on plant regeneration. *Biol. Plant.*, 2003/4, **47**, 179–183.
13. Tomida, S., Hanai, T., Honda, H. and Kobayashi, T., Analysis of expression profile using fuzzy adaptive resonance theory. *Bioinformatics*, 2002, **18**, 1703–1083.
14. Larkin, P. J. and Scowcroft, W. R., Somaclonal variation – A novel source of variability from cell cultures for plant improvement. *Theor. Appl. Genet*., 1981, **60**, 197–214.
15. Albiol, J., Campmajo, C., Casas, C. and Poch, M., Biomass estimation in plant cell cultures: a neural network approach. *Biotechnol. Prog*., 1995, **11**, 88 –92.
16. Honda, H., Takikawa, N., Noguchi, H., Hanai, T. and Kobayashi, T., Image analysis associated with a fuzzy neural network and estimation of shoot length of regenerated rice callus. *J. Ferment. Bioeng*., 1997, **84**, 342–347.

ACKNOWLEDGEMENTS. Financial assistance from CSIR to V.S.S.P. as SRF is acknowledged.

Received 30 December 2003; revised accepted 10 March 2004

Cloning and characterization of the *DMC1* genes in *Oryza sativa*

Shalaka S. Metkar, Jayashree K. Sainis* and Suresh K. Mahajan

Molecular Biology Division, Bhabha Atomic Research Centre, Mumbai 400 085, India

The *DMC1* gene is a major homologous recombination gene, expressed during prophase I of meiosis. We have isolated and analysed two *DMC1* genes, viz. type A and type B from rice. It was observed that *DMC1* type A is located on chromosome 12 whereas *DMC1* type B is on chromosome 11. The location of *DMC1* type A in the region on chromosome 12 that is duplicated on rice chromosome 11 is a new finding in this report. Earlier *DMC1* orthologues have been reported on chromosomes 9 and 11. Partially overlapping 5′ and 3′ cDNAs of one of the *DMC1* genes were obtained and used to generate the full-length *DMC1* gene, which was cloned and over-expressed in *E. coli*.

GENETIC recombination is a fundamental process in living cells. Studies on homologous recombination have potential applications in gene targeting[1,2] and in the development of apomictic varieties in plants like rice[3]. A number of plant recombination genes have been reported recently[4]. One of these is *DMC1*, which was identified in *S. cerevisiae* as a meiosis-specific homologue of the *E. coli recA* gene[5], required for recombination, synaptonemal complex formation and cell cycle progression[6] and later shown to be present in several mammalian, fungal and plant species[7]. The protein products [Dmc1] of the yeast *DMC1* and its human and basidiomycetes orthologues have been shown to possess biochemical properties similar to the bacterial RecA[8–10]. Plant *DMC1* orthologues have been identified in *Lilium longiflorum*[11,12], *Arabidopsis thaliana*[13,14], *Hordeum vulgare* (GenBank Accession Number AF234170), *Glycine max* (GenBank Accession Number U66836) and *Oryza sativa*[3,15,16], but so far there is no report on the characterization of any plant Dmc1 protein.

The important role of the *DMC1* genes during meiosis was demonstrated by gene expression analysis in meiotic tissue using RT–PCR, Northern blot and *in situ* hybridization in lily, *A. thaliana* and rice[3,12,14,17]. Immunofluorescence localization of the DMC1 (LIM15) protein in the leptotene and zygotene stages of meiosis prophase I was observed in lily[18,19]. The important role of this gene during meiosis was confirmed with the characterization of the *DMC1* mutant of *A. thaliana*[20]. This mutant showed drastically aberrant chromosome behaviour in prophase I; bivalent formation by pairing of homologous chromosomes was impaired and the ten univalent chromosomes

*For correspondence. (e-mail: jksainis@magnum.barc.ernet.in)